Evolution of the macromolecular structure of sporopollenin during thermal degradation

S. Bernard, K. Benzerara, O. Beyssac, E. Balan, G.E. Brown Jr.

Heliyon

CrossMark

Evolution of the macromolecular structure of sporopollenin during thermal degradation

S. Bernard [a],*, **K. Benzerara [a]**, **O. Beyssac [a]**, **E. Balan [a]**, **G.E. Brown Jr. [b,c]**

[a] *Institut de Minéralogie, de Physique des Matériaux, et de Cosmochimie (IMPMC), Sorbonne Universités - MNHN, UPMC Univ Paris 06, CNRS UMR 7590, IRD UMR 206, 75005 Paris, France*

[b] *Surface & Aqueous Geochemistry Group, Department of Geological and Environmental Sciences, Stanford University, Stanford, CA 94305-2115, USA*

[c] *Department of Photon Science and Stanford Synchrotron Radiation Lightsource, SLAC National Accelerator Laboratory, 2575 Sand Hill Road, Menlo Park, CA 94025, USA*

* Corresponding author.

E-mail address: sbernard@mnhn.fr (S. Bernard).

Abstract

Reconstructing the original biogeochemistry of organic microfossils requires quantifying the extent of the chemical transformations they experienced during burial and maturation processes. In the present study, fossilization experiments have been performed using modern sporopollenin chosen as an analogue for the resistant biocompounds possibly constituting the wall of many organic microfossils. Sporopollenin powder has been processed thermally under argon atmosphere at different temperatures (up to 1000 °C) for varying durations (up to 900 min). Solid residues of each experiment have been characterized using infrared, Raman and synchrotron-based XANES spectroscopies. Results indicate that significant defunctionalisation and aromatization affect the molecular structure of sporopollenin with increasing temperature. Two distinct stages of evolution with temperature are observed: in a first stage, sporopollenin experiences dehydrogenation and deoxygenation simultaneously (below 500 °C); in a second stage (above 500 °C) an increasing concentration in aromatic groups and a lateral growth of aromatic layers are observed. With increasing heating

duration (up to 900 min) at a constant temperature (360 °C), oxygen is progressively lost and conjugated carbon–carbon chains or domains grow progressively, following a log-linear kinetic behavior. Based on the comparison with natural spores fossilized within metasediments which experienced intense metamorphism, we show that the present experimental simulations may not perfectly mimic natural diagenesis and metamorphism. Yet, performing such laboratory experiments provides key insights on the processes transforming biogenic molecules into molecular fossils.

Keywords: Earth sciences, Organic geochemistry, Micro fossils, Preservation of fossils, Biomolecules

1. Introduction

Inferring the original biochemical composition of fossils has been a long-standing goal. A major difficulty resides in the poor quality of the biogeochemical signals preserved in the fossil record: in addition to the impact of bio-alteration, the increase of temperature and pressure associated with burial (a.k.a. diagenesis) inevitably alters the original biochemical signatures of fossilized organic molecules (e.g., Briggs, 2003; Briggs and Summons, 2014). The general paleobiological perception has long been that burial-induced biomolecule degradation processes are detrimental to the preservation of biomolecular signatures in ancient rocks. Yet, a number of fossil occurrences has been reported in metamorphic rocks of various ages and facies, including high-grade metamorphism: greenschist facies conditions (e.g., Knoll and Ohta, 1988; Kidder and Awramik, 1990; Knoll, 1992; Molyneux, 1998; Powell, 2003; Kempe et al., 2005; Butterfield et al., 2007), amphibolite facies (e.g., Franz et al., 1991; Pestal et al., 1999; Hanel et al., 1999; Squire et al., 2006; Zang, 2007; Schiffbauer et al., 2007), or blueschist facies (e.g., Johnston et al., 1987; Bernard et al., 2007, 2010a; Galvez et al., 2012a,b).

Quantifying the extent of the transformations induced by burial processes transforming biogenic molecules into molecular fossils requires experimental simulations. A number of authors have attempted to experimentally mimic fossilization processes (e.g., Briggs and Kear, 1993; Briggs, 1995; Grimes et al., 2001; Brock et al., 2006; Gupta et al., 2006, 2007, 2009; Yin et al., 2007; Sansom et al., 2010; Cunningham et al., 2012; Picard et al., 2015). Recently, Ruhl et al. (2011),Schiffbauer et al. (2012), Watson et al. (2012), Fraser et al. (2014) and Li et al. (2014) have exposed modern green alga (*Botryococcus braunii*), fossilized acritarchs, clubmoss spores (*Lycopodium clavatum*) and modern bacteria (*Escherichia coli*) to experimental conditions mimicking diagenesis and documented the chemical changes of the organic compounds of these objects using spectroscopy and spectrometry techniques. All these studies have demonstrated that morphological and molecular biosignatures may be

preserved in some contexts, at least partially. Yet, the molecular and structural transformations of organics occurring during burial-induced diagenesis remain poorly constrained.

Following these recent works, we report here results of thermal degradation experiments performed on sporopollenin from *Lycopodium clavatum* spores to simulate advanced diagenesis processes. The chemical evolution of sporopollenin compounds during thermal treatments has already been the focus of a number of studies (e.g., Sengupta, 1975, 1977; Rouxhet et al., 1979; Bestougeff et al., 1985; Hayatsu et al., 1988; Ayache and Oberlin, 1990; Hemsley et al., 1996; Yule et al., 2000; Watson et al., 2012; Fraser et al., 2014). Because of its intrinsic resistance against chemical and biological agents, the exact molecular structure of sporopollenin remains debated (Hemsley et al., 1993; de Leeuw et al., 2006; Moore et al., 2006; Vandenbroucke and Largeau, 2007). Sporopollenin has been proposed to be a biomacromolecule essentially composed of polyalkyls (Guilford et al., 1988; Hayatsu et al., 1988), a mixture of aliphatic and aromatic moieties (Wehling et al., 1989; Meychik et al., 2006) or predominantly aromatic moieties (de Leeuw et al., 2006). Rather than a unique substance, sporopollenin may encompass a variety of related biopolymers, containing varying amounts of oxygen, in the form of ketone, hydroxyl, carboxylic, ester and ether groups (de Leeuw et al., 2006; Bernard et al., 2009; Fraser et al., 2012). Noteworthy, sporopollenin constitutes an important component of the selectively-preserved sedimentary organic record (e.g., Tegelaar et al., 1989; Briggs, 1999 Derenne and Largeau, 2001; de Leeuw et al., 2006; Vandenbroucke and Largeau, 2007; Zonneveld et al., 2010) and can be chemically preserved, at least partially, in rocks having experienced diagenetic conditions (e.g., Hemsley et al., 1996; Cody et al., 1996; Bernard et al., 2009; Steemans et al., 2010; Fraser et al., 2012) and, in some cases, intense metamorphic conditions (Bernard et al., 2007).

In the present study, sporopollenin has been exposed to thermal treatment in open crucibles under argon atmosphere at different temperatures (up to 1000 °C) for different durations (up to 900 min). The solid residues of all experiments have been characterized using infrared, Raman and synchrotron-based X-ray absorption near edge structure (XANES) spectroscopies. We interpret the differences in the XANES spectra of experimentally thermally altered sporopollenin collected at the C K-edge as resulting from molecular and structural transformations. We then compare the C-XANES data collected on these experimental samples with C-XANES data collected *in situ*, at the submicrometer scale, on natural fossilized spores using synchrotron-based scanning transmission X-ray microscopy (STXM). Finally, we highlight the importance of conducting such experiments for the search for ancient life in the geological record.

2. Material and methods

2.1. Material

Sporopollenin was purchased from Polyscience, Inc. As specified by the manufacturer, this sporopollenin powder was separated from common clubmoss *(Lycopodium clavatum)* microspores by successive treatments with solvents, caustic (sodium hydroxide), and acids (acetic anhydride and sulphuric acid) to remove the inner cellulose wall, i.e. the endospore. *Lycopodium clavatum* sporopollenin has been classically used in a number of studies (Cody et al., 1996; Hemsley et al., 1996; Yule et al., 2000; Watson et al., 2012; Fraser et al., 2014) and can be seen as a generic analogue of sporopollenin compounds.

Experimental heat-treated sporopollenin residues are compared hereafter with metamorphic sporopollenin composing the wall of organic fossils of lycophyte megaspores preserved in 230-Myr-old (Triassic) metasedimentary carbonate concretions from the Vanoise massif (Western Alps, France) that experienced blueshist facies metamorphism (~360 °C, ~14kbars, i.e. a burial depth of about 40 km) during the Alpine orogeny (Bernard et al., 2007, 2010a).

2.2. Thermal treatment

A first set of 5 experiments has consisted in heating sporopollenin powder samples at 250 °C, 360 °C, 500 °C, 750 °C and 1000 °C for 90 min in an inert Argon atmosphere. To test the impact of the experiment duration, two additional experiments have been performed at 360 °C for 9 and 900 min, respectively. For all experiments, the increase of temperature followed a constant ramp of 5 °C.min^{-1}. The elemental composition of the solid residues for each experiment has been estimated via thermal combustion analyses (Service Central d'Analyse - CNRS) while chemical, structural and molecular signatures have been investigated by infrared, Raman and XANES spectroscopies.

2.3. Infrared spectroscopy

Infrared spectroscopy data have been collected at IMPMC using a Nicolet FTIR 6700 spectrometer equipped with a globar source and a KBr beam splitter. The absorption of the infrared beam by the samples has been measured from 400 to 4000 cm^{-1} in the diffuse reflectance mode,with a spectral resolution of 2 cm^{-1}, using a DLATGS pyroelectric detector. Additional conventional transmission measurements performed on the same samples diluted in a KBr matrix have provided similar spectra over the investigated range and have thus attested the reliability of this diffuse reflectance configuration.

2.4. Raman spectroscopy

Raman data have been obtained using a Renishaw INVIA microspectrometer operating at IMPMC as described in Bernard et al. (2008). Spectra have been measured from 500 to 3500 cm^{-1} at constant room temperature using the 514.5 nm wavelength of a 100 mW Modulaser Argon laser (green laser) focused on the sample through a Leica DMLM microscope with a 50X objective (NA = 0.75). This configuration yields a horizontal resolution of ~1 μm for a laser power delivered at the sample surface set at around 0.25 mW to prevent irreversible thermal damage that could be due to laser-induced heating (Beyssac et al., 2003a). Light is dispersed by a grating with 1800 lines/mm and the signal was analyzed with a RENCAM CCD detector. Measurements have been performed with a circularly polarized laser using a 1/4 wavelength plate placed before the microscope in order to limit polarization effects.

2.5. XANES spectroscopy

Soft X-ray XANES spectroscopy coupled with scanning transmission X-ray microscopy (STXM) is increasingly used to characterize natural kerogens and detect the preservation of original biomolecules within fossilized organisms (e.g., Boyce et al., 2002; Bernard et al., 2007, 2009, 2010a; Lepot et al., 2008 Lepot et al., 2011; Cody et al., 2011; Galvez et al., 2012a,b). Importantly, radiation damage per unit of analytical information has been shown to be typically 100–1000 times lower in STXM-based XANES spectroscopy compared to TEM-based EELS (Rightor et al., 1997; Braun et al., 2005, 2009; Hitchcock et al., 2008). XANES measurements have been carried out at the C K-edge on the STXM Polymer beamline 5.3.2.2. (Kilcoyne et al., 2003) and on the Molecular Environmental Science STXM beamline 11.0.2.2 (Bluhm et al., 2006) at the Advanced Light Source (Berkeley, USA). The electron current in the storage ring is held constant in top-off mode at 500 mA at a storage ring energy of 1.9 GeV. Energy calibration was accomplished using the well-resolved 3p Rydberg peak at 294.96 eV of gaseous CO_2 for the C K-edge. C-XANES data were collected following the procedures for X-ray microscopy studies of radiation sensitive samples recommended by Wang et al. (2009). Samples have been finely ground, suspended in water and deposited on Si_3N_4 windows. C-XANES spectra have been measured over the 280 to 330 eV energy range (C K-edge), using a step size of 0.3 eV between 280 and 283 eV, 0.1 eV between 283 and 295 eV and 0.3 eV between 295 and 330 eV, with a theoretical energy resolution better than 100 meV. The collected C-XANES spectra of heat-treated sporopollenin have been normalized to the total amount of carbon (measured by the edge step between the pre-edge region (270–280 eV) and the post-edge region (320–340 eV)) using the Athena software package (Ravel and Newville, 2005).

To facilitate the interpretation of the spectral evolution of sporopollenin with increasing heating duration or temperature, C-XANES data have been decomposed using an arctangent function to model the absorption edge and Gaussian functions following the procedure described in Bernard et al. (2010b) (Fig. 4). The center position, the amplitude and the width of the arctangent function are fixed to 291.5, 1.0 and 0.4 eV, respectively. Although the natural lineshape of a XANES peak is a Lorentzian function, Gaussian functions have been used to take into account instrumental broadening effects (Braun et al., 2006). Each Gaussian function had a fixed energy position and a constant width (0.4 eV below 295 eV and 2 eV above). The broad peak at 285 eV has been decomposed into four Gaussian functions, accounting for resonances by different multiple carbon–carbon bond species as previously shown by Braun et al. (2006) and Bernard et al. (2010b). Following Bernard et al. (2012) and Le Guillou et al. (2013, 2014),), the parameter S_A is defined as the contribution of the areas under Gaussian functions accounting for the aromatic contribution (peak at ~285 eV) relative to total carbon content and can thus be seen as a parameter directly related to the aromaticity. A second parameter, S_O, is defined as the sum of the areas of the Gaussian functions centered at 286.7, 287.2, 288.6 and 289.2 eV accounting, respectively, for the contribution of ketone, phenol or alcohol, carboxylic and hydroxyl groups, relative to the total carbon content. It should be kept in mind that these parameters do not correspond to absolute concentrations, as (1) the oscillator strengths of the different electronic transitions are different and not precisely known and as (2) some of the Gaussians functions used for the present deconvolution of XANES signals do not account for the absorption of given functional groups, but for broad spectral features corresponding to highly delocalized excited states sometimes referred to as 1s→σ* virtual state transitions or the overlapping contribution of Feshbach resonances (Stöhr, 1992).

3. Results

3.1. Elemental composition

Elemental compositions of solid residues are shown in a Van Krevelen diagram (Fig. 1). The solid residues of the thermal degradation experiments performed in the present study can be considered as a maturation series. Two stages of evolution with increasing temperature can be distinguished: a first stage below 500 °C during which both O/C and H/C ratios decrease with increasing temperature; and a second stage above 500 °C and up to 1000 °C during which only the H/C ratios continue to decrease while O/C ratios remain constant (Fig. 1). At 1000 °C, sporopollenin has likely already experienced the onset of dry gas generation as indicated by the H/C and O/C ratios (Bernard et al., 2010c). With increasing experimental durations at 360 °C, sporopollenin
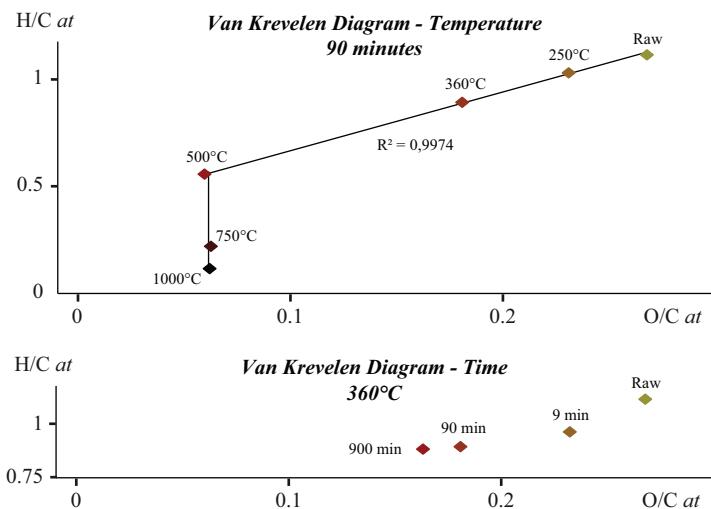
Fig. 1. Van Krevelen diagrams showing the evolution of H/C and O/C atomic ratios of organic residues of sporopollenin heat-treated at different temperature for 90 min (top) and of organic residues of sporopollenin heat-treated at 360 °C for different experimental durations (bottom).

residues follow a singular path in the Van Krevelen diagram: both H/C and O/C ratios decrease with increasing time, H/C ratios decreasing first more rapidly than O/C ratios as observed in short duration experiments and then less rapidly as observed in longer duration experiments (Fig. 1).

3.2. Infrared spectroscopy

The evolution with increasing temperature of the infrared spectra of sporopollenin evidences the chemical degradation of this biopolymer (Fig. 2). Qualitatively, hydroxyl groups (OH vibration, $\sim$3450 cm^{-1}) first disappear at about 360 °C. Carbonyl groups (C = O vibration, $\sim$ 1710 cm^{-1}) disappear at 500 °C. Aliphatic CH groups ($\sim$1350 cm^{-1}, 1450 cm^{-1} and $\sim$2900 cm^{-1}) are still observed at 500 °C, although their absorption is low. Concomitantly with this loss of oxygenated and hydrogenated aliphatic functions, aromatic groups ($\sim$700 to 900 cm^{-1} and $\sim$3050 cm^{-1}) become predominant within residues of sporopollenin heat-treated at 500 °C. At temperatures above 500 °C, the residues reflect totally the beam, preventing collection of IR data.

3.3. Raman spectroscopy

The very high fluorescence overwhelming the Raman signal (using the 514.5 nm ArgonLaser) prevents collecting data on sporopollenin heat-treated at temperatures lower than 500 °C. Above 500 °C, the evolution of the Raman spectra of sporopollenin with increasing temperature shows the structural evolution of this biopolymer (Fig. 2). The first-order region in the Raman

A. Infrared Spectra
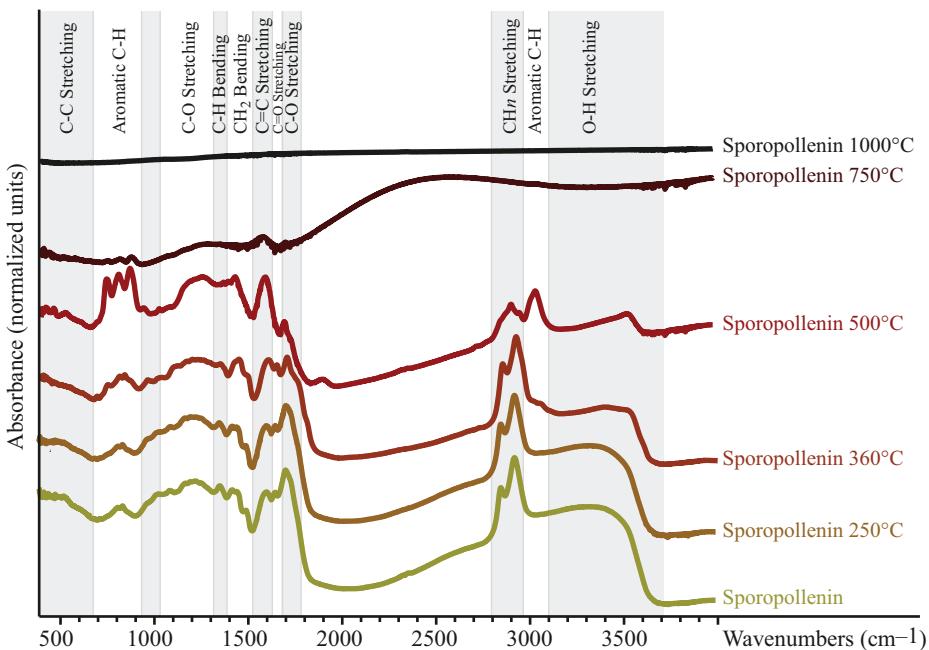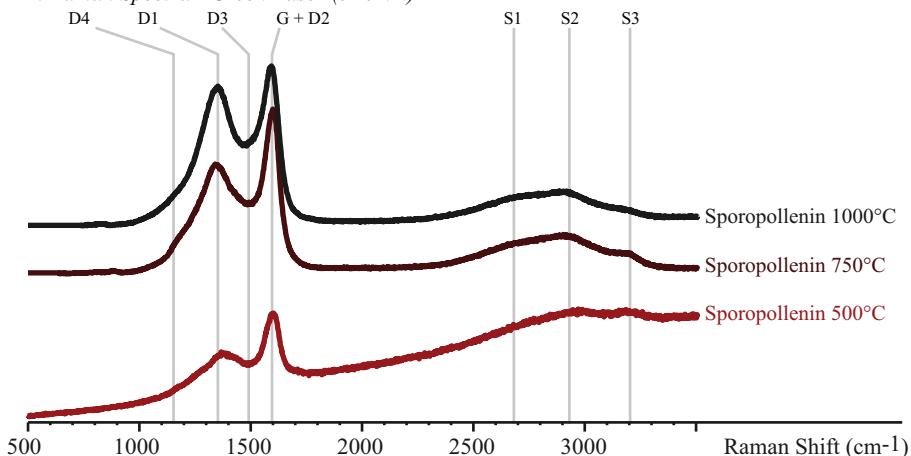
Fig. 2. Infrared (top) and Raman (bottom) spectra of organic residues of sporopollenin heat-treated up to 1000 °C for 90 min.

spectra of heat-treated sporopollenin displays defect bands D1, D3 and D4 at ~1350, 1500 and 1250 cm^{-1}, respectively, as well as a slightly asymmetric band comprising the G and the D2 bands at ~1600 cm^{-1}. With increasing temperature, from 500 °C to 1000 °C, the G band becomes a bit more asymmetric towards high wave-numbers and the intensity of the D1 band increases while the intensities of the D3 and D4 bands slightly decrease. This evolution results in a decrease of the overall area of the main defect band (D1) relatively to the G band. Three Raman bands are observed in the second-order region as very broad

features: the S1 band at ~2700 cm^{-1}, the S2 band at ~2950 cm^{-1} and the S3 at ~3200 cm^{-1}. From 500 °C to 1000 °C, these bands do not significantly evolve.

3.4. XANES spectroscopy

3.4.1. C-XANES spectrum of sporopollenin

The C-XANES spectrum of sporopollenin indicates that this biopolymer is mostly composed of: (1) aromatic carbon groups (the peak at 285.1 eV is interpreted as 1s→p* transitions in aromatic or olefinic carbon (C=C); the peak at 292.8 eV is indexed as 1s→σ* transitions in aromatic C–C) and (2) oxygen-containing carbon functional groups (features at 286.7, 287.2, 288.6 and 289.2 eV) (Fig. 3). The 286.7 eV peak is assigned to 1s→π* transitions in ketone (C=O) functional groups while the 288.6 eV peak is assigned to 1s→π* transitions in carboxylic functional groups (Cody et al., 1996). The gentle absorption feature at 289.2 eV is interpreted as 1s→π* transitions in hydroxyl groups (C–OH) while the barely distinguishable shoulder centered at 287.2 eV (1s→π* transitions) is indicative of phenol (Ar–OH) or alcohol (C–OH) functional groups (Boyce et al., 2002; Bernard et al., 2009).

3.4.2. Temperature experiments

In contrast to infrared and Raman spectroscopies, C-XANES spectroscopy allows following the chemical and structural evolution of sporopollenin over the whole range of experimental temperatures of the present study, from room temperature to 1000 °C (Fig. 3). With increasing temperature, the absorption peaks corresponding to oxygen-containing functional groups progressively decrease, alcohol and phenol groups being the first to disappear between 250 and 360 °C, followed by ketone groups at 500 °C, while some carboxylic groups may remain in the structure up to 1000 °C (Fig. 3). In parallel, the absorption feature centered at 285.1 eV, revealing the presence of aromatic or olefinic groups, broadens and increases in intensity from room temperature up to 750 °C (Fig. 3). At 1000 °C, this absorption feature shifts from 285.1 to 285.4 eV, concomitantly with the appearance of an absorption peak at 292.8 eV (corresponding to 1s→σ* transitions of aromatic groups). No sharp 1s→σ* exciton at 291.7 eV, related to the presence of extensive planar domains of highly conjugated aromatic layers (Ahuja et al., 1996; Bernard et al., 2010b), can be observed in the XANES spectrum of sporopollenin heat-treated at 1000 °C.

3.4.3. Time experiments

At 360 °C, the duration of the experimental heating has a clear impact on the molecular structure of sporopollenin (Fig. 3). The evolution of the C-XANES
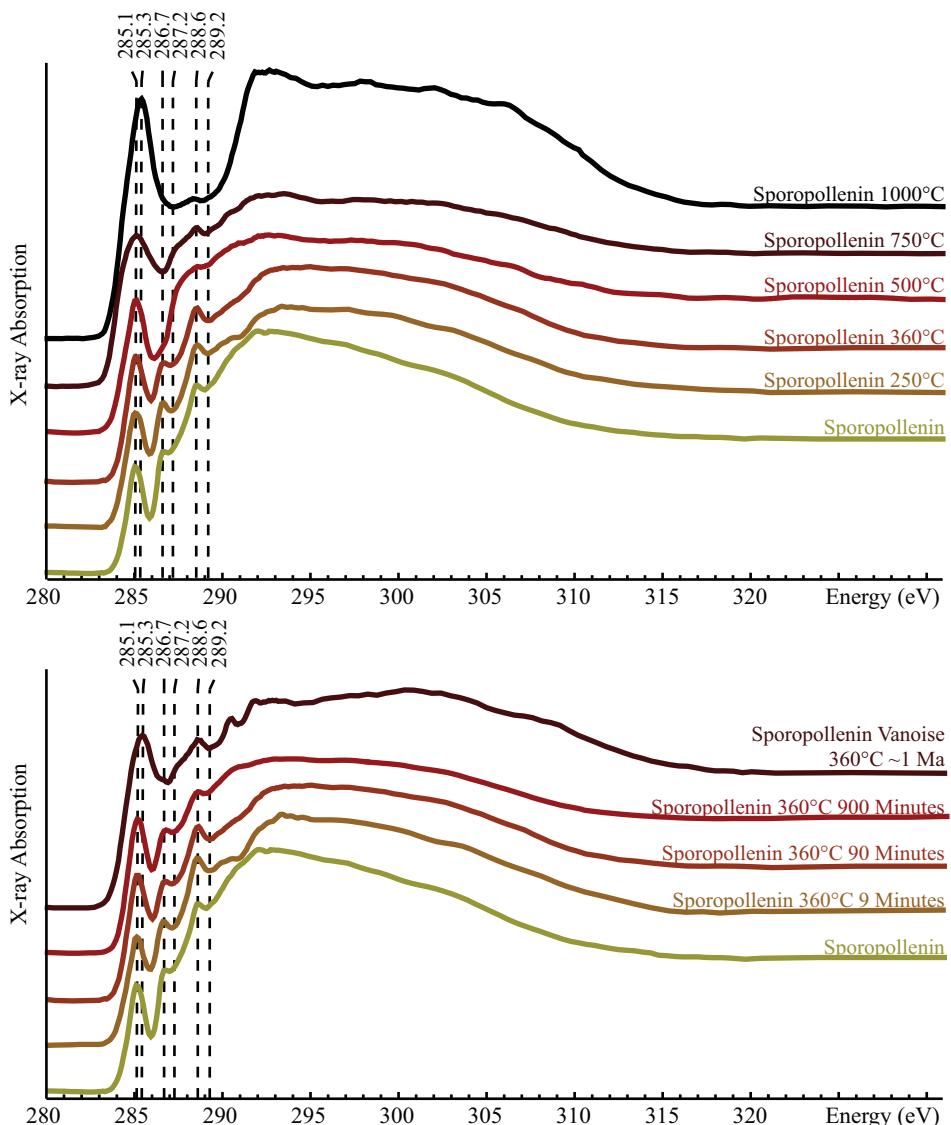
Fig. 3. C-XANES of organic residues of sporopollenin heat-treated up to 1000 °C for 90 min (top) and at 360 °C for different durations up to 900 min (bottom). The C-XANES spectrum of metamorphic sporopollenin from Vanoise (Bernard et al., 2007) is shown for comparison. Peaks at 285.1 (and 285.3), 286.7, 287.2, 288.6 and 289.2 are attributed to electronic transitions of carbon involved in aromatic or olefinic groups, ketonic or phenolic groups, phenolic groups, carboxylic groups and hydroxylated groups, respectively.

spectra collected on solid residues with increasing experiment duration appears qualitatively similar to the evolution with increasing temperature (Fig. 3). The absorption peaks attributed to oxygen-containing C-functional groups progressively decrease in intensity, while the absorption feature due to the presence of aromatic or olefinic C-groups broadens and increases in intensity (Fig. 3). Even for the longest experiment (900 min), no sharp 1s→σ* exciton at 291.7 eV is observed.

X-ray Absorption

285.1
285.3
286.7
287.2
288.6
289.2

1

0

280   285   290   295   300   305   310   Energy (eV)

S_O
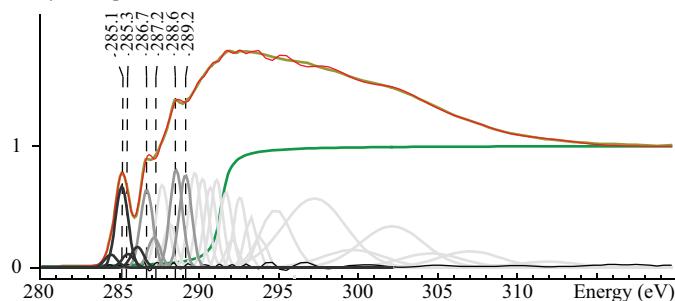
Oxygen Functions vs Temperature

2.5
2.4
2.3
2.2
2.1
2.0

0   200   400   Temperature (°C)   800   1000

◆ *Heat-treated Sporopollenin*
× *Vanoise Sporopollenin*

S_A
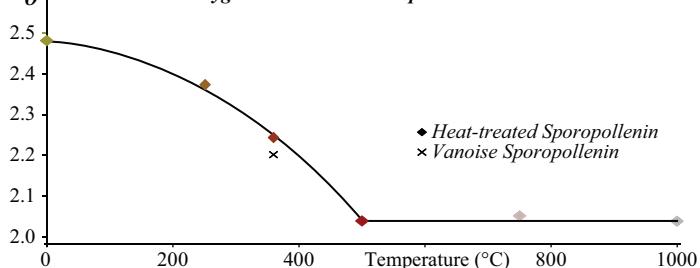
Aromaticity vs Temperature

3.0
2.5
2.0
1.5
1.0

0   200   400   Temperature (°C)   800   1000

R² = 0,9999

R² = 0,9994

S_O

Oxygen Content vs Time

2.5
2.4
2.3
2.2
2.1
2.0

0   100   Duration of pyrolysis at 360°C (in minutes)   900   ~1 Ma

R² = 0,9848

Aromaticity vs Time

2.5

S_A

1.6
1.4
1.2
1.0

0   100   Duration of pyrolysis at 360°C (in minutes)   900   ~1 Ma

R² = 0,9978
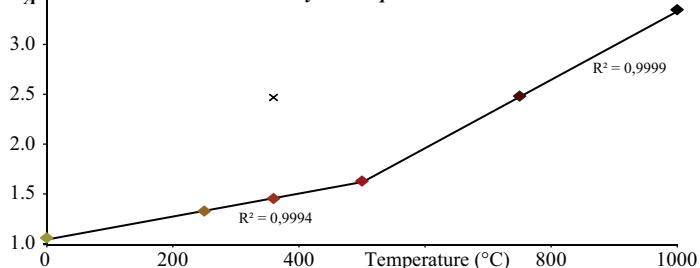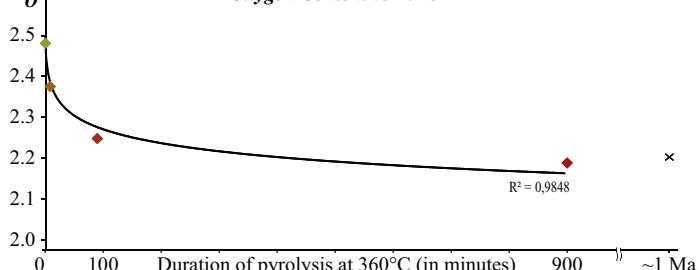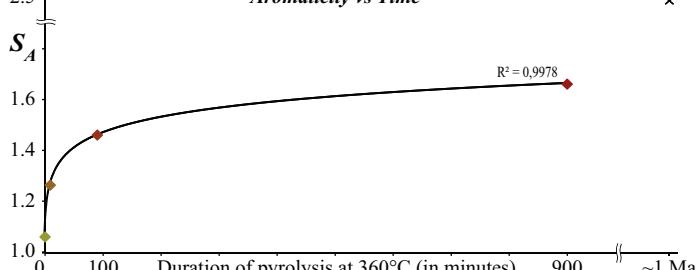
3.4.4. Evolution of S_A and S_O parameters with increasing temperature and heating duration

As shown in Fig. 4, the S_A and S_O parameters of experimentally heat-treated sporopollenin evolve differently with increasing temperature. After a nonlinear decrease from room temperature to 500 °C, the S_O values reach a plateau and remain constant between 500 and 1000 °C. This threshold value of 2 for the S_O parameter corresponds to a negligible concentration in oxygen functions as shown by bulk elemental analyses. In contrast, the S_A values increase continuously and linearly with temperature from room temperature to 1000 °C, with a slope three times higher between 500 and 1000 °C than between room temperature and 500 °C. With increasing heating duration, the S_A values of experimental sporopollenin increase while the S_O values decrease. Both S_A and S_O values follow logarithmic laws with experimental durations (Fig. 4).

3.4.5. Comparison with natural samples

The C-XANES spectrum of metamorphic sporopollenin from Vanoise which experienced a maximum temperature of 360 °C and a maximum pressure of 14 kbars for at least 1 Myr (Bernard et al., 2007) is shown in Fig. 3. Noteworthy, this spectrum is very similar to the spectrum of sporollenin experimentally heat-treated at 750 °C for 90 min in terms of peak positions, widths and intensities, as illustrated by their S_A and S_O values (2.47 and 2.2. for the Vanoise metamorphic sporopollenin *versus* 2.48 and 2.07 for sporopollenin heat-treated at 750 °C for 90 min, respectively). In contrast, extrapolating the logarithmic laws modeling the evolution of the S_A and S_O values of sporopollenin heat-treated at 360 °C with time for durations of 1 Myr leads to S_A and S_O values of 3.29 and 1.37 (< 2), respectively, which do not match the S_A and S_O values of metamorphic sporopollenin from Vanoise.

4. Discussion

4.1. Influence of temperature: oxygen loss and aromatization

The present study shows the main changes in the molecular structure of sporopollenin with increasing thermal maturation: oxygen-containing functional groups are progressively lost, while the relative abundance of aromatic structures increases within the solid residue. These findings appear consistent with the significant defunctionalisation evidenced by previous experimental studies of thermal degradation of sporopollenin at relatively low temperatures

Fig. 4. Fitting procedure of the C-XANES spectra of organic residues of heat-treated sporopollenin as detailed in the text (top) and (below) graphs showing the evolution of the S_A and S_O parameters with increasing temperature and with increasing experiment duration.

(Rouxhet et al., 1979; Hemsley et al., 1996; Yule et al., 2000; Watson et al., 2012; Fraser et al., 2014). Two different stages of evolution can be identified from room temperature to 1000 °C. The data reported here indicate that during thermal treatment below 500 °C, sporopollenin experiences carbonization (Vandenbroucke and Largeau, 2007). The evolution of the O/C and H/C atomic ratios below 500 °C suggests that the removal of a large proportion of oxygenated functions likely occurred as a loss of CO_2, mainly, and H_2O (Vandenbroucke and Largeau, 2007). Alcohol and phenol groups are the first to disappear between 250 and 360 °C, followed by ketone groups at 500 °C. Such loss of O-containing molecules yields a nearly pure and poorly ordered carbon phase highly concentrated in hydrocarbon generating structures. Interestingly, the rate of oxygen loss increases with increasing temperature, while the rate of aromatic carbon enrichment is constant, suggesting enrichment in polyalkyl carbons, consistent with observations reported by Watson et al. (2012) and Fraser et al. (2014) on residues of sporopollenin having experienced thermal treatments in closed systems and under vacuum.

Above 500 °C, the total oxygen content remains constant and negligible (as indicated by bulk analyses and confirmed by the S_O values), while the S_A values still increase linearly with temperature, even faster than below 500 °C. The H/C atomic ratio of the residual kerogen decreases during this phase, suggesting generation of hydrocarbons as C_nH_{2n+2} molecules (Vandenbroucke and Largeau, 2007). The net increase of S_A values, the appearance of an absorption peak at 292.8 eV and the concomitant shift of the aromatic peak maximum absorption energy from 285.1 to 285.4 eV reflect an increasing concentration in aromatic groups as well and a lateral growth of aromatic layers (Bernard et al., 2010b). The formation of planar domains of highly conjugated π systems, which provide a particularly stable electronic configuration (Cody et al., 2008), might indeed influence electron delocalization and thus the appearance of an excitonic effect associated with the broad 1s→π* absorption feature at ~285 eV (Ahuja et al., 1996; Bernard et al., 2010b). However, no sharp 1s→σ* exciton at 291.7 eV can be observed in the XANES spectrum of sporopollenin heat-treated at 1000 °C. The absence of such absorption feature is not surprising as graphitizing carbons start to display it only after an experimental heat treatment above 1600 °C (Bernard et al., 2010b) and suggests that the aromatic cluster size of sporopollenin residue has not significantly increased within the studied range of temperatures. This appears consistent with the slight evolution of the Raman signal with increasing temperature.

4.2. Influence of experimental duration

The present study also provides some insights on the influence of heating duration on organic molecule thermal alteration processes. It has been anticipated from

carbonization /graphitization experiments that longer periods of heating would likely result in increasingly ordered carbonaceous materials (e.g., Bestougeff et al., 1985; Newell et al., 1996; Beyssac et al., 2003b; Cody et al., 2008; Zhao et al., 2010; Schiffbauer et al., 2012). The C-XANES data of heat-treated sporopollenin residues confirm that the level of carbonization increases with increasing duration of thermal treatment at 360 °C: oxygen-containing functional groups are progressively lost while the relative abundance of aromatic structures increases. However, the fact that S_O and S_A values co-vary with time indicates that pericondensation of aromatic rings remains incomplete even for the longest experimental duration. The absence of a sharp 1s→σ* exciton at 291.7 eV, related to the presence of extensive planar domains of highly conjugated aromatic layers (Ahuja et al., 1996; Cody et al., 2008; Bernard et al., 2010b), suggests that the aromatic cluster size of sporopollenin residue has not significantly increased over the studied range of experimental durations. In contrast to what occurs in natural settings, at such a "low" temperature, sporopollenin appears to only experience the first steps of carbonization.

Interestingly, in contrast to their evolution with temperature, S_O and S_A values exhibit a log-linear relationship with thermal treatment duration. Such log-linear evolution cannot be described using the algebraic expressions of functions of the most common reaction mechanisms operating in solid-state reactions (Aboulkas et al., 2010; Kebukawa et al., 2010). Similar log-linear behaviors have been reported for parameters describing the evolution of maturation/degradation/ graphitization degree of carbonaceous materials as a function of experiment durations (e.g., Newell et al., 1996; Beyssac et al., 2003b; Zhao et al., 2010; Kebukawa et al., 2010; Schiffbauer et al., 2012). Of note, the increase of the exciton intensity in XANES spectra of extraterrestrial insoluble organic matter experiencing experimental graphitization under flash heating also exhibits a log-linear behavior with time (Cody et al., 2008). The chemical and structural transformation of organic macromolecules with increasing thermal treatment duration presumably involves a highly cooperative, multi-step process, involving considerable bond breaking, bond migration and bond rearrangement (e.g., Cody et al., 2008). As oxygen is progressively lost and conjugated carbon–carbon chains or domains progressively grow, more steps may become necessary with increasing time for continued domain growth and oxygen loss, leading to the observed log-linear kinetic behavior (Cody et al., 2008). This log-linear relationship likely evolves into linear correlations for long durations as proposed by Beyssac et al. (2003b), which may explain the apparent discrepancies between experimental and natural samples.

4.3. Discrepancies with natural samples

Extrapolating laboratory results to natural processes remains difficult (e.g., Li et al., 2014). As geological time cannot be replicated in the laboratory,

the question arises whether or not laboratory experiments such as the ones performed in the present study really mimic processes taking place in natural settings and provide a valuable insight into the fate of biological material during burial and diagenesis. The chemical reactions that occur during organic maturation are usually described by a nearly first order kinetic law, with a rate constant related to temperature by the Arrhenius equation, whereby high temperature and short duration experiments should produce results equivalent to a low temperature and long duration experiment (e.g. Vandenbroucke and Largeau, 2007). Thus, temperatures and heating rates considerably higher than those encountered in nature have to be applied to the rock samples to compensate for long geological time periods (e.g., Lewan et al., 1979; Behar et al., 1997, 2010; Seewald et al., 1998).

Interestingly, when plotted in a Van Krevelen diagram, the solid residues of heat-treated sporopollenin do not follow the mean evolution pathways of kerogen type II but two different stages of evolution (Fig. 1). While the second stage (above 500 °C) is only characterized by a decrease of H/C ratios (O/C ratios remain constant), both O/C and H/C ratios of sporopollenin residues decrease at the same time with increasing temperature during the first stage (below 500 °C), indicating that dehydrogenation and deoxygenation occur simultaneously. This result differs from what happens during natural carbonization process, i.e. a decrease of O/C ratios followed by a decrease of H/C ratios with increasing temperature (e.g., Vandenbroucke and Largeau, 2007). As suggested by Ayache and Oberlin (1990), dehydrogenation might have been favored by the low heating rate and pressure at which the present experiments were conducted.

Here, the Raman spectrum of sporopollenin experimentally heat-treated at 750 °C for 90 min appears similar to spectra of natural soots or charcoals, while its C-XANES spectrum is similar to the one of Vanoise metamorphic sporopollenin which has experienced 360 °C (Bernard et al., 2007, 2010a). In addition, extrapolations of the logarithm laws of S_A and S_O values at 360 °C for long durations do not match the S_A and S_O values of the metamorphic sporopollenin from Vanoise. This inconsistency illustrates the difficulty to properly simulate fossilization processes in the laboratory. Of note, thermal degradation experiments do not simulate biodegradation processes that might occur in natural settings. Some (or most) of the observed differences might thus result from the early diagenetic biodegradation experienced by fossilized sporopollenin compounds. Yet, sporopollenin compounds have been shown to be highly resistant to biodegradation. Therefore, the discrepancies observed here between experimental and natural samples might not be attributed to such processes. In contrast, these discrepancies may reside in the fact that the present experiments have been performed on pure sporopolleninin open crucibles under

an inert gas flow at atmospheric pressure with a slow heating rate while Vanoise sporopollenin has experienced 360 °C and 14kbars for ~1 Myr during the Alpine orogeny (Bernard et al., 2007, 2010a). Indeed, pressure has been shown to be a key factor in the rate at which the decomposition of kerogen proceeds and may favor aromatization and the degree of saturation of the maturation products (Ayache and Oberlin, 1990; Beyssac et al., 2003b; Vandenbroucke and Largeau, 2007). Oxygen fugacity conditions may also impact the molecular transformations of sporopollenin (Yule et al., 2000; Twiddle and Bunting, 2010; Schiffbauer et al., 2012; Jardine et al., 2015). In addition, organic maturation processes may also be strongly affected by the presence of water and minerals in low-temperature systems (Huang, 1996; Seewald et al., 2000; Pan et al., 2009; Lewan and Roy, 2011).

In any case, consistently with results by Bestougeff et al. (1985), Cody et al. (1996), Yule et al. (2000), Watson et al. (2012) and Fraser et al. (2014), the present study evidences that the thermal evolution of sporopollenin is not a continuous, single phase process, and should instead be seen as the result of different processes involving sequential dehydration and dehydrogenation leading to a progressively aromatized bio/geopolymer. Thus, although the evolution of sporopollenin documented here may not exactly reflect the chemical changes that take place during diagenesis in natural settings, it evidences that the thermal evolution of any organic macromolecule should not be seen as a progressive modification of a single initial substance but as a sequence of degradation and formation/condensation reactions.

4.4. Implications for the reconstruction of the original biochemical composition of organic microfossils

Most of the witnesses of the first chapters of the history of life are unicellular organic-walled microfossils which fall into the category of "acritarchs" (e.g., Servais, 1996; Knoll, 2014). The term 'acritarch' was first introduced by Evitt (1963) to describe "small microfossils of unknown and probably varied biological affinities, consisting of a central cavity enclosed by a wall of single or multiple layers and of chiefly organic composition". Various biological affinities and evolutionary patterns have been proposed for acritarchs. Hence, among acritarchs have been described unicellular photosynthetic protists such as spores, cysts of green algae or dinoflagellates, cyanobacterial envelopes, heterotrophic protists, pellicles of euglenids or even egg-cases of copepod-like crustaceans (e.g., Colbath and Grenfell, 1995; Servais, 1996; Arouri et al., 2000; Butterfield, 2005; Marshall et al., 2005; Kempe et al., 2005; Javaux and Marshal, 2006; Huntley et al., 2006; Knoll et al., 2006; Moczydłowska and Willman, 2009; Sergeev, 2009; Taylor and Strother, 2009; Javaux et al., 2010; Strother et al., 2011; Battison and Brasier, 2012; Knoll, 2014).

The experiments reported in the present study have been performed on sporopollenin compounds which do not embrace all the possible original chemical compositions of organic-walled acritarchs. A number of extant organic-walled microalgae and dinocysts have been shown to be composed of highly resistant biomolecules that differ from sporopollenin compounds, such as algaenans or dinosporins. Algaenan compounds have been described as highly aliphatic unbranched (but crosslinked) carbon chains, while dinosporin compounds can be seen as crosslinked carbohydrate-based polymers (Kokinos et al., 1998; Versteegh and Blokker, 2004; de Leeuw et al., 2006; Kodner et al., 2009; Versteegh et al., 2012). Similarly to sporopollenins, these resistant macromolecules should not be seen as unique substances, but rather as series of biomolecules. In any case, these compounds may behave differently from sporopollenin during burial. Additional experiments should thus be performed on such compounds to provide a more complete view of the transformations having potentially been experienced by organic-walled acritarchs during the geological history of their host rocks and hence eventually allow reconstructing their original biochemical compositions.

5. Conclusion

The trends in chemical and structural changes of sporopollenin during thermal degradation reported here can be seen as a new milestone towards a generalized mechanistic model for the evolution of the spectroscopic signatures of natural biogenic organic matter during burial and diagenetic processes, which appears as a pre-requisite to properly reconstruct the original chemistry of fossils. Yet, the present experimental simulations do not seem to perfectly mimic the processes occurring in natural settings. In addition to investigating the impact of biodegradation in the laboratory, future studies should focus on quantifying the influence of key parameters such as oxygen fugacity conditions and the geochemical nature of the fluid and the mineral matrix on the extent of biomolecule degradation occuring during fossilization processes. Additional experiments also need to be performed using different organic precursors in order to more completely embrace the possible original compositions of organic microfossils found in the geological record.

Declarations

Author contribution statement

Sylvain Bernard: Conceived and designed the experiments; Performed the experiments; Analyzed and interpreted the data; Contributed reagents, materials, analysis tools or data; Wrote the paper.

Competing interest statement

The authors declare no conflict of interest.

Additional information

No additional information is available for this paper.

References

Aboulkas, A., El Harfi, E., El Bouadili, A., 2010. Thermal degradation behaviors of polyethylene and polypropylene. Part I: Pyrolysis kinetics and mechanisms. Energ. Convers. Manage. 51, 1363–1369.

Ahuja, R., Bruhwiler, P.A., Wills, J.M., Johansson, B., Martensson, N., Eriksson, O., 1996. Theoretical and experimental study of the graphite 1s X-ray absorption edges. Phys. Rev. B 54 (20), 14396–14404.

Arouri, K.R., Greenwood, P.F., Walter, M.R., 2000. Biological affinities of Neoproterozoic acritarchs from Australia: microscopic and chemical characterisation. Org. Geochem. 31 (1), 75–89.

Ayache, J., Oberlin, A., 1990. Thermal simulations of the evolution of carbonaceous oil-source rocks as compared with pyrolysis of model substances of types I, II and III. J. Anal. Appl. Pyrol. 17, 329–356.

Battison, L., Brasier, M.D., 2012. Remarkably preserved prokaryote and eukaryote microfossils within 1 Ga-old lake phosphates of the Torridon Group, NW Scotland. Precambrian Res. 196-197, 204–217.

Behar, F., Roy, S., Jarvie, D., 2010. Artificial maturation of a Type I kerogen in closed system: Mass balance and kinetic modelling. Org. Geochem. 41 (11), 1235–1247.

Behar, F., Vandenbroucke, M., Tang, Y., Marquis, F., Espitalie, J., 1997. Thermal cracking of kerogen in open and closed systems: Determination of kinetic parameters and stoichiometric coefficients for oil and gas generation. Org. Geochem. 26 (5-6), 321–339.

Bernard, S., Benzerara, K., Beyssac, O., Brown Jr., G.E., 2010a. Multiscale characterization of pyritized plant tissues in blueschist facies metamorphic rocks. Geochim. Cosmochim. Ac. 74, 5054–5068.

Bernard, S., Benzerara, K., Beyssac, O., Brown, G.E., Stamm, L.G., Duringer, P., 2009. Ultrastructural and chemical study of modern and fossil sporoderms by Scanning Transmission X-ray Microscopy (STXM). Rev. Palaeobot. Palyno. 156 (1-2), 248–261.

Bernard, S., Benzerara, K., Beyssac, O., Menguy, N., Guyot, F., Brown, G.E., Goffe, B., 2007. Exceptional preservation of fossil plant spores in high-pressure metamorphic rocks. Earth Planet. Sc. Lett. 262 (1-2), 257–272.

Bernard, S., Beyssac, O., Benzerara, K., 2008. Raman Mapping Using Advanced Line-Scanning Systems: Geological Applications. Appl. Spectrosc. 62 (11), 1180–1188.

Bernard, S., Beyssac, O., Benzerara, K., Findling, N., Brown Jr., G.E., 2010b. XANES, Raman and XRD signatures of anthracene-based cokes and saccharose-based chars submitted to high temperature pyrolysis. Carbon 48, 2506–2516.

Bernard, S., Horsfield, B., Schulz, H.-M., Schreiber, A., Wirth, R., Vu, T.T.A., Perssen, F., Könitzer, S., Volk, H., Sherwood, N., Fuentes, D., 2010c. Multi-scale detection of organic and inorganic signatures provides insights into gas shale properties and evolution. Chem. Erde 70 (Suppl. 3), 119–133.

Bernard, S., Horsfield, B., Schulz, H.-M., Wirth, R., Schreiber, A., Sherwood, N., 2012. Geochemical evolution of organic-rich shales with increasing maturity: A STXM and TEM study of the Posidonia Shale (Lower Toarcian, northern Germany). Mar. Petrol. Geol. 31 (1), 70–89.

Bestougeff, M.A., Byramjee, R.J., Pesneau, B., 1985. On the chemical mechanism of kerogen thermal transformation. Study of the transformation of sporopollenin. Org. Geochem. 8 (6), 389–398.

Beyssac, O., Brunet, F., Petitet, J.P., Goffe, B., Rouzaud, J.N., 2003b. Experimental study of the microtextural and structural transformations of carhonaceous materials under pressure and temperature. Eur. J. Mineral. 15 (6), 937–951.

Beyssac, O., Goffe, B., Petitet, J.P., Froigneux, E., Moreau, M., Rouzaud, J.N., 2003a. On the characterization of disordered and heterogeneous carbonaceousmaterials by Raman spectroscopy. Spectrochim. Acta A 59 (10), 2267–2276.

Bluhm, H., Andersson, K., Araki, T., Benzerara, K., Brown, G.E., Dynes, J.J., Ghosal, S., Gilles, M.K., Hansen, H.C., Hemminger, J.C., Hitchcock, A.P., Ketteler, G., Kilcoyne, A.L.D., Kneedler, E., Lawrence, J.R., Leppard, G.G., Majzlam, J., Mun, B.S., Myneni, S.C.B., Nilsson, A., Ogasawara, H., Ogletree, D.F., Pecher, K., Salmeron, M., Shuh, D.K., Tonner, B., Tyliszczak, T., Warwick, T., Yoon, T.H., 2006. Soft X-ray microscopy and spectroscopy at the molecular environmental science beamline at the Advanced Light Source. J. Electron Spectrosc. 150 (2-3), 86–104.

Boyce, C.K., Cody, G.D., Feser, M., Jacobsen, C., Knoll, A.H., Wirick, S., 2002. Organic chemical differentiation within fossil plant cell walls detected with X-ray spectromicroscopy. Geology 30 (11), 1039–1042.

Braun, A., Huggins, F.E., Kelly, K.E., Mun, B.S., Ehrlich, S.N., Huffman, G.P., 2006. Impact of ferrocene on the structure of diesel exhaust soot as probed with wide-angle X-ray scattering and C(1s) NEXAFS spectroscopy. Carbon 44 (14), 2904–2911.

Braun, A., Huggins, F.E., Shah, N., Chen, Y., Wirick, S., Mun, S.B., Jacobsen, C., Huffman, G.P., 2005. Advantages of soft X-ray absorption over TEM-EELS for solid carbon studies a comparative study on diesel soot with EELS and NEXAFS. Carbon 43 (1), 117–124.

Braun, A., Kubatova, A., Wirick, S., Mun, S., 2009. Radiation damage from EELS and NEXAFS in diesel soot and diesel soot extracts. J. Electron Spectrosc. 170 (1-3), 42–48.

Briggs, D.E.G., 1995. Experimental taphonomy. Palaios 10 (6), 539–550.

Briggs, D.E.G., 2003. The role of decay and mineralization in the preservation of soft-bodied fossils. Annu. Rev. Earth Pl. Sc. 31, 275–301.

Briggs, D.E.G., Kear, A.J., 1993. Fossilization of soft-tissue in the laboratory. Science 259 (5100), 1439–1442.

Briggs, D.E.G., Summons, R.E., 2014. Ancient biomolecules: Their origins, fossilization, and role in revealing the history of life. Bioessays 36 (5), 482–490.

Brock, F., Parkes, R.J., Briggs, D.E.G., 2006. Experimental pyrite formation associated with decay of plant material. Palaios 21 (5), 499–506.

Butterfield, N.J., 2005. Probable Proterozoic fungi. Paleobiology 31 (1), 165–182.

Butterfield, N.J., Balthasar, U., Wilson, L.A., 2007. Fossil diagenesis in the burgess shale. Palaeontology 50, 537–543.

Cody, G.D., Alexander, C., Yabuta, H., Kilcoyne, A., Araki, T., Ade, H., Dera, P., Fogel, M., Militzer, B., Mysen, B., 2008. Organic thermometry for chondritic parent bodies. Earth Planet Sc. Lett. 272 (1-2), 446–455.

Cody, G.D., Botto, R.E., Ade, H., Wirick, S., 1996. The application of soft X-ray microscopy to the in-situ analysis of sporinite in coal. Int. J. Coal Geol. 32 (1-4), 69–86.

Cody, G.D., Gupta, N.S., Briggs, D.E.G., Kilcoyne, A.L.D., Summons, R.E., Kenig, F., Plotnick, R.E., Scott, A.C., 2011. Molecular signature of chitin-protein complex in Paleozoic arthropods. Geology 39 (3), 255–258.

Colbath, G.K., Grenfell, H.R., 1995. Review of biological affinities of Paleozoic acid-resistant, organic-walled eukaryotic algal microfossils (including "acritarchs"). Rev. Palaeobot. Palyno. 86, 287–314.

Cunningham, J.A., Thomas, C.W., Bengtson, S., Marone, F., Stampanoni, M., Turner, F.R., Bailey, J.V., Raff, R.A., Raff, E.C., Donoghue, P.C.J., 2012. Doushantuo fossils: Implications for the interpretation of the embryo-like Ediacaran. Philos. T. Roy. Soc. B 279, 1857–1864.

de Leeuw, J.W., Versteegh, G.J.M., van Bergen, P.F., 2006. Biomacromolecules of algae and plants and their fossil analogues. Plant Ecol. 182 (1-2), 209–233.

Derenne, S., Largeau, C., 2001. A review of some important families of refractory macromolecules: composition,origin, and fate in soils and sediments. Soil Sci. 166 (11), 833–847.

Evitt, W.R., 1963. A discussion and proposals concerning fossil dinoflagellates, hystrichospheres, and acritarchs I. P. Natl. Acad. Sci. 49, 158–164.

Franz, G., Mosbrugger, V., Menge, R., 1991. Carbo-permian Pteridophyll Leaf fragments from an amphibolite facies basement, Tauern Window, Austria. Terra Nova 3 (2), 137–141.

Fraser, W.T., Scott, A.C., Forbes, A.E.S., Glasspool, I.J., Plotnick, R.E., Kenig, F., Lomax, B.H., 2012. Evolutionary stasis of sporopollenin biochemistry revealed by unaltered Pennsylvanian spores. New Phytol. 196, 397–401.

Fraser, W.T., Watson, J.S., Sephton, M.A., Lomax, B.H., Harrington, G., Gosling, W.D., Self, S., 2014. Changes in spore chemistry and appearance with increasing maturity. Rev. Palaeobot. Palyno. 201, 41–46.

Galvez, M.E., Beyssac, O., Benzerara, K., Bernard, S., Menguy, N., Cox, S.C., Martinez, I., Johnston, M.R., Brown Jr., G.E., 2012a. Morphological preservation of carbonaceous plant fossils in high grade metamorphic rocks from New Zealand. Geobiology 10 (2), 118–129.

Galvez, M.E., Beyssac, O., Benzerara, K., Menguy, N., Bernard, S., Cox, S.C., 2012b. Micro and nano-textural evidence of Ti(-Ca-Fe) mobility during fluid-rock interactions in carbonaceous lawsonite-bearing rocks from New Zealand. Contr. Mineral. Petrol. 164 (5), 891–895.

Grimes, S.T., Brock, F., Rickard, D., Davies, K.L., Edwards, D., Briggs, D.E., Parkes, R.J., 2001. Understanding fossilization: Experimental pyritization of plants. Geology 29 (2), 123–126.

Guilford, W.J., Schneider, D.M., Labovitz, J., Opella, S.J., 1988. High-resolution Solid-state C-13 NMR-spectroscopy of Sporopollenins From Different Plant Taxa. Plant Physiol. 86 (1), 134–136.

Gupta, N.S., Cody, G.D., Tetlie, O.E., Briggs, D.E., Summons, R.E., 2009. Rapid incorporation of lipids into macromolecules during experimental decay of invertebrates: Initiation of geopolymer formation. Org. Geochem. 40 (5), 589–594.

Gupta, N.S., Michels, R., Briggs, D.E.G., Collinson, M.E., Evershed, R.P., Pancost, R.D., 2007. Experimental evidence for the formation of geomacromolecules from plant leaf lipids. Org. Geochem. 38 (1), 28–36.

Gupta, N.S., Michels, R., Briggs, D.E.G., Evershed, R.P., Pancost, R.D., 2006. The organic preservation of fossil arthropods: an experimental study. Proc. R. Soc. B Biol. Sci. 273 (1602), 2777–2783.

Hanel, M., Montenari, M., Kalt, A., 1999. Determining sedimentation ages of high-grade metamorphic gneisses by their palynological record: a case study in the Northern Schwarzwald (Variscan Belt, Germany). Int. J. Earth Sci. 88 (1), 49–59.

Hayatsu, R., Botto, R.E., McBeth, R.L., Scott, R.G., Winans, R.E., 1988. Chemical alteration of a biological polymer "sporopollenin" during coalification:

origin, formation, and transformation of the coal maceral sporinite. Energ. Fuel. 2 (6), 843–847.

Hemsley, A.R., Barrie, P.J., Chaloner, W.G., Scott, A.C., 1993. The composition of sporopollenin and its use in living and fossil plant systematics. Grana 32 (Suppl. 1), 2–11.

Hemsley, A.R., Scott, A.C., Barrie, P.J., Chaloner, W.G., 1996. Studies of fossil and modern spore wall biomacromolecules using C-13 solid state NMR. Ann. Bot. 78 (1), 83–94.

Hitchcock, A.P., Dynes, J.J., Johansson, G., Wang, J., Botton, G., 2008. Comparison of NEXAFS microscopy and TEM-EELS for studies of soft matter. Micron 39 (3), 311–319.

Huang, W.L., 1996. Experimental study of vitrinite maturation: effects of temperature, time, pressure, water, and hydrogen index. Org. Geochem. 24 (2), 233–241.

Huntley, J.W., Xiao, S.H., Kowalewski, M., 2006. 1.3 Billion years of acritarch history: An empirical morphospace approach. Precambrian Res. 144 (1-2), 52–68.

Jardine, P.E., Fraser, W.T., Lomax, B.H., Gosling, W.D., 2015. The impact of oxidation on spore and pollen chemistry. J. Micropalaeontol. 34, 139–149.

Javaux, E.J., Marshal, C.P., 2006. A new approach in deciphering early protist paleobiology and evolution: Combined microscopy and microchemistry of single Proterozoic acritarchs. Rev. Palaeobot. Palyno. 139 (1-4), 1–15.

Javaux, E.J., Marshall, C.P., Bekker, A., 2010. Organic-walled microfossils in 3.2-billion-year-old shallow-marine siliciclastic deposits. Nature 463 (7283), 934–938.

Johnston, R., Raine, J., Watters, W., 1987. Drumduan Group of East Nelson, New Zealand: plant-bearing Jurassic arc rocks metamorphosed during terrane interaction. J. Roy. Soc. New Zeal. 17 (3), 275–301.

Kebukawa, Y., Nakashima, S., Zolensky, M.E., 2010. Kinetics of organic matter degradation in the Murchison meteorite for the evaluation of parent-body temperature history. Meteorit. Planet. Sci. 45 (1), 99–113.

Kempe, A., Wirth, R., Altermann, W., Stark, R.W., Schopf, J.W., Heckl, W.M., 2005. Focussed ion beam preparation and in situ nanoscopic study of Precambrian acritarchs. Precambrian Res. 140 (1-2), 36–54.

Kidder, D.L., Awramik, S.M., 1990. Acritarchs in lower greenschist facies argillite of the middle Proterozoic Libby Formation, Upper Belt Supergroup, Montana. Palaios 5, 124–133.

Kilcoyne, A.L.D., Tyliszczak, T., Steele, W.F., Fakra, S., Hitchcock, P., Franck, K., Anderson, E., Harteneck, B., Rightor, E.G., Mitchell, G.E., Hitchcock, A.P., Yang, L., Warwick, T., Ade, H., 2003. Interferometer-controlled scanning transmission X-ray microscopes at the Advanced Light Source. J. Synchrotron Radiat. 10, 125–136.

Knoll, A.H., 1992. Vendian microfossils in metasedimentary cherts of the Scotia group, Prins Karls Forland, Svalbard. Palaeontology 35, 751–774.

Knoll, A.H., 2014. Paleobiological Perspectives on Early Eukaryotic Evolution. Cold Spring Harb. Perspect. Biol. 6 (1), a016121.

Knoll, A.H., Ohta, Y., 1988. Microfossils in metasediments from Prins Karls Forland, Western Svalbard. Polar Res. 6, 59–67.

Knoll, A.H., Javaux, E.J., Hewitt, D., Cohen, P., 2006. Eukaryotic organisms in Proterozoic oceans. Philos.Trans. R. Soc. B Biol. Sci. 361 (1470), 1023–1038.

Kodner, R., Knoll, A.H., Summons, R.E., 2009. Phylogenetic investigation of the aliphatic, non-hydrolyzable biopolymer algaenan, with a focus on the green algae. Org. Geochem. 40, 854–862.

Kokinos, J.P., Eglinton, T.I., Goñi, M.A., Boon, J.J., Martoglio, P.A., Anderson, D.M., 1998. Characterisation of a highly resistant biomacromolecular material in the cell wall of a marine dinoflagellate resting cyst. Org. Geochem. 28, 265–288.

Le Guillou, C., Remusat, L., Bernard, S., Brearley, A.J., Leroux, H., 2013. Amorphization and D/H fractionation of kerogens during experimental electron irradiation: comparison with chondritic organic matter. Icarus 226, 101–110.

Le Guillou, C., Bernard, S., Brearley, A.J., Remusat, L., 2014. Evolution of organic matter in Orgueil, Murchison and Renazzo during parent body aqueous alteration: In situ investigations. Geochim. Cosmochim. Ac. 131, 368–392.

Lepot, K., Benzerara, K., Philippot, P., 2011. Biogenic versus metamorphic origins of diverse microtubes in 2.7 Gyr old volcanic ashes: Multi-scale investigations. Earth Planet. Sc. Lett. 312 (1-2), 37–47.

Lewan, M.D., Roy, S., 2011. Role of water in hydrocarbon generation from Type-I kerogen in Mahogany oil shale of the Green River Formation. Org. Geochem. 42 (1), 31–41.

Lewan, M.D., Winters, J.C., McDonald, J.H., 1979. Generation of oil-like pyrolyzates from organic-rich shales. Science 203 (4383), 897–899.

Li, J., Bernard, S., Benzerara, K., Beyssac, O., Allard, T., Cosmidis, J., Moussou, J., 2014. Impact of biomineralization on the preservation of microorganisms during fossilization: An experimental perspective. Earth Planet. Sc. Lett. 400, 113–122.

Marshall, C.P., Javaux, E.J., Knoll, A.H., Walter, M.R., 2005. Combined micro-Fourier transform infrared (FTIR) spectroscopy and micro-Raman spectroscopy of Proterozoic acritarchs: a new approach to palaeobiology. Precambrian Res. 138, 208–224.

Meychik, N.R., Matveyeva, N.P., Nikolaeva, Y.I., Chaikova, A.V., Yermakov, I.P., 2006. Features of ionogenic group composition in polymeric matrix of lily pollen wall. Biochemistry-Moscow 71 (8), 893–899.

Moczydłowska, M., Willman, S., 2009. Ultrastructure of cell walls in ancient microfossils as a proxy to their biological affinities. Precambrian Res. 173, 27–38.

Molyneux, S.G., 1998. An upper Dalradian microfossil reassessed. J. Geol. Soc. 155, 741–743.

Moore, S.E.M., Hemsley, A.R., French, A.N., Dudley, E., Newton, R.P., 2006. New insights from MALDI-ToF MS, NMR, and GC-MS: mass spectrometry techniques applied to palynology. Protoplasma 228 (1-3), 151–157.

Newell, J.A., Edie, D.D., Fuller Jr., E.L., 1996. Kinetics of carbonization and graphitization of PBO Fiber. J. Appl. Polym. Sci. 60, 825–832.

Pan, C.C., Geng, A.S., Zhong, N.N., Liu, J.Z., Yu, L.P., 2009. Kerogen pyrolysis in the presence and absence of water and minerals: Amounts and compositions of bitumen and liquids. Fuel 88 (5), 909–919.

Pestal, G., Brüggemann-Ledolter, M., Draxler, I., Eibinger, D., Eichberger, H., Reiter, C., Scevik, F., Fritz, A., Koller, F., 1999. Ein Vorkommen von Oberkarbon in den mittleren Hohen Tauern. Jb. Geol. B.-A. 141, 491–502.

Picard, A., Kappler, A., Schimd, G., Quaroni, L., Obst, M., 2015. Experimental diagenesis of organo-mineral structures formed by microaerophilic Fe(II)-oxidizing bacteria. Nat. Commun. 6, 6277.

Powell, W., 2003. Greenschist-facies metamorphism of the Burgess Shale and its implications for models of fossil formation and preservation. Can. J. Earth Sci. 40 (1), 13–25.

Ravel, B., Newville, M., 2005. ATHENA, ARTEMIS, HEPHAESTUS: data analysis for X-ray absorption spectroscopy using IFEFFIT. J. Synchrotron Radiat. 12 (4), 537–541.

Rightor, E.G., Hitchcock, A.P., Ade, H., Leapman, R.D., Urquhart, S.G., Smith, A.P., Mitchell, G., Fischer, D., Shin, H.J., Warwick, T., 1997. Spectromicroscopy of poly(ethylene terephthalate): Comparison of spectra and radiation damage rates in x-ray absorption and electron energy loss. J. Phys. Chem. B 101 (11), 1950–1960.

Rouxhet, P.G., Villey, M., Oberlin, A., 1979. Infrared study of the pyrolysis products of sporopollenin and lignite. Geochim. Cosmochim. Ac. 43 (11), 1705–1713.

Ruhl, I.D., Salmon, E., Hatcher, P.G., 2011. Early diagenesis of Botryococcus braunii race A as determined by high resolution magic angle spinning (HRMAS) NMR. Org. Geochem. 42, 1–14.

Sansom, R.S., Gabbott, S.E., Purnelli, M.A., 2010. Non-random decay of chordate characters causes bias in fossil interpretation. Nature 463, 797–800.

Schiffbauer, J.D., Wallace, A.F., Hunter Jr., J.L., Kowalewski, M., Bodnar, R.J., Xiao, S.H., 2012. Thermally-induced structural and chemical alteration of organic-walled microfossils: an experimental approach to understanding fossil preservation in metasediments. Geobiology 10, 402–423.

Schiffbauer, J.D., Yin, L.M., Bodnar, R.J., Kaufman, A.J., Meng, F.W., Hu, J., Shen, B., Yuan, X.L., Bao, H.M., Xiao, S.H., 2007. Ultrastructural and geochemical characterization of archean-paleoproterozoic graphite particles: Implications for recognizing traces of life in highly metamorphosed rocks. Astrobiology 7 (4), 684–704.

Seewald, J.S., Benitez-Nelson, B.C., Whelan, J.K., 1998. Laboratory and theoretical constraints on the generation and composition of natural gas. Geochim. Cosmochim. Ac. 62 (9), 1599–1617.

Seewald, J.S., Eglinton, L.B., Ong, Y.L., 2000. An experimental study of organic-inorganic interactions during vitrinite maturation. Geochim. Cosmochim. Ac. 64 (9), 1577–1591.

Sengupta, S., 1975. Experimental alterations of the spores of lycopodium clavatum as related to diagenesis. Rev. Palaeobot. Palyno. 19 (3), 173–192.

Sengupta, S., 1977. A comparative study of the gradual degradation of exines, resulting from the effects of temperature. Rev. Palaeobot. Palyno. 24 (5), 239–246.

Sergeev, V.N., 2009. The distribution of microfossil assemblages in Proterozoic rocks. Precambrian Res. 173, 212–222.

Servais, T., 1996. Some considerations on acritarch classification. Rev. Palaeobot. Palyno. 93, 9–22.

Squire, R.J., Stewart, I.R., Zang, W.L., 2006. Acritarchs in polydeformed and highly altered Cambrian rocks in western Victoria. Aust. J. Earth Sci. 53 (5), 697–705.

Steemans, P., Lepot, K., Marshall, C.P., Le Hérissé, A., Javaux, E.J., 2010. FTIR characterisation of the chemical composition of Silurian miospores (cryptospores and trilete spores) from Gotland, Sweden. Rev. Palaeobot. Palyno. 162, 577–590.

Stöhr, J., 1992. NEXAFS Spectroscopy. Springer Series in Surface Science. Springer-Verlag, Berlin, pp. 291.

Strother, P.K., Battison, L., Brasier, M.D., Wellman, C.H., 2011. Earth's earliest non-marine eukaryotes. Nature 473, 505–509.

Taylor, W.A., Strother, P.K., 2009. Ultrastructure, morphology, and topology of Cambrian palynomorphs from the Lone Rock Formation, Wisconsin, USA. Rev. Palaeobot. Palyno. 153, 296–309.

Tegelaar, E., de Leeuw, J., Derenne, S., Largeau, C., 1989. A reappraisal of kerogen formation. Geochim. Cosmochim. Ac. 53 (11), 3103–3106.

Twiddle, C.L., Bunting, M.J., 2010. Experimental investigations into the preservation of pollen grains: A pilot study of four pollen types. Rev. Palaeobot. Palyno. 162, 621–630.

Vandenbroucke, M., Largeau, C., 2007. Kerogen origin, evolution and structure. Org. Geochem. 38 (5), 719–833.

Versteegh, G.J.M., Blokker, P., 2004. Resistant macromolecules of extant and fossil microalgae. Phycol. Res. 52, 325–339.

Versteegh, G.J.M., Blokker, P., Bogus, K.A., Harding, I.C., Lewis, J., Oltmanns, S., Rochon, A., Zonneveld, K.A.F., 2012. Infra red spectroscopy, flash pyrolysis, thermally assisted hydrolysis and methylation (THM) in the presence of tetramethylammonium hydroxide (TMAH) of cultured and sediment-derived Lingulodinium polyedrum (Dinoflagellata) cyst walls. Org. Geochem. 43, 92–102.

Wang, J., Morin, C., Li, L., Hitchcock, A., Scholl, A., Doran, A., 2009. Radiation damage in soft X-ray microscopy. J. Electron Spectrosc. 170 (1-3), 25–36.

Watson, J.S., Fraser, W.T., Sephton, M.A., 2012. Formation of a polyalkyl macromolecule from the hydrolysable component within sporopollenin during heating/pyrolysis experiments with Lycopodium spores. J. Anal. Appl. Pyrol. 95, 138–144.

Wehling, K., Niester, C., Boon, J.J., Willemse, M.T.M., Wiermann, R., 1989. p-Coumaric acid- a monomer in the sporopollenin skeleton. Planta 179, 376–380.

Yin, L., Zhu, M., Knoll, A.H., Yuan, X., Zhang, J., Hu, J., 2007. Doushantuo embryos preserved inside diapause egg Cysts. Nature 446, 661–663.

Yule, B.L., Roberts, S., Marshall, J.E.A., 2000. The thermal evolution of sporopollenin. Org. Geochem. 31 (9), 859–870.

Zang, W.L., 2007. Deposition and deformation of late Archaean sediments and preservationof microfossils in the Harris Greenstone Domain, Gawler Craton, South Australia. Precambrian Res. 156 (1-2), 107–124.

Zhao, Y., Wei, F., Yu, Y., 2010. Effects of reaction time and temperature on carbonization in asphaltene pyrolysis. J. Petrol Sci. Eng. 74, 20–25.

Zonneveld, K.A.F., Versteegh, G.J.M., Kasten, S., Eglinton, T.I., Emeis, K.C., Huguet, C., Koch, B.P., de Lange, G.J., de Leeuw, J.W., Middelburg, J.J., Mollenhauer, G., Prahl, F.G., Rethemeyer, J., Wakeham, S.G., 2010. Selective preservation of organic matter in marine environments, processes and impact on the sedimentary record. Biogeosciences 7 (2), 483–511.